DOI: 10.1002/chem.200801758

Functionalization of Carbon Nanotubes with Water-Insoluble Porphyrin in Ionic Liquid: Direct Electrochemistry and Highly Sensitive Amperometric Biosensing for Trichloroacetic Acid

Wenwen Tu, Jianping Lei,* and Huangxian Ju*[a]

Abstract: A functional composite of single-walled carbon nanotubes (SWNTs) with hematin, a water-insoluble porphyrin, was first prepared in 1-butyl-3-methylimidazolium hexafluorophosphate ([BMIM][PF_6]) ionic liquid. The novel composite in ionic liquid was characterized by scanning electron microscopy, ultraviolet absorption spectroscopy, and electrochemical impedance spectroscopy, and showed a pair of direct redox peaks of the Fe^{III}/Fe^{II} couple. The composite–[BMIM][PF_6]-modified glassy carbon electrode showed excellent electrocatalytic activity toward the reduction of trichloroacetic acid (TCA) in neutral media due to the synergic effect among SWNTs, [BMIM][PF_6], and porphyrin, which led to a highly sensitive and stable amperometric biosensor for TCA with a linear range from 9.0×10^{-7} to 1.4×10^{-4} M. The detection limit was 3.8×10^{-7} M at a signal-to-noise ratio of 3. The TCA biosensor had good analytical performance, such as rapid response, good reproducibility, and acceptable accuracy, and could be successfully used for the detection of residual TCA in polluted water. The functional composite in ionic liquid provides a facile way to not only obtain the direct electrochemistry of water-insoluble porphyrin, but also construct novel biosensors for monitoring analytes in real environmental samples.

Keywords: biosensors · carbon nanotubes · ionic liquids · porphyrinoids · trichloroacetic acid

Introduction

Trichloroacetic acid (TCA), as an organohalide pollutant, is of major environmental concern due to its extensive use in agriculture and public health programs.[1] Urinary TCA has been proposed as a biomarker of chronic ingestion exposure to nonvolatile haloacetic acids from chlorinated drinking water.[2,3] Thus, the World Health Organization has urgently appealed for the development of rapid, reliable, and accurate analytical methods for the detection of TCA.[4] Currently, TCA is generally measured by gas chromatography with precolumn trap enrichment and microwave plasma emission detection,[5] headspace gas chromatography with electron capture or mass spectrometric detection,[6,7] and high-performance liquid chromatography with solid-phase microextraction and electrospray mass spectrometric detection.[8] Although these methods have adequate sensitivity, they suffer from the need for expensive equipment, time-consuming derivatization and extraction processes, and professional operation. Particularly, it is difficult to use these methods for in situ or online monitoring.

To solve these problems, electrochemical biosensors based on electrodes modified with hemin/Nafion,[9] myoglobin/poly(styrenesulfonate),[10] and hemoglobin/clay[11] have been developed for the detection of TCA. However, the sensitivity of these biosensors is relatively poor. With the great progress made in nanoscience and nanotechnology,[12–16] some nanomaterials, such as $CaCO_3$ nanoparticles,[17] colloidal gold nanoparticles,[18] and zirconium phosphate nanosheets,[19] have been employed in immobilizing hemoglobin or myoglobin to improve the sensitivity of amperometric biosensors for TCA. However, the sensitizing efficiency is limited, and most of them can detect TCA only in a narrow concentration range. Moreover, the possible activity change of immobilized proteins upon long-term storage affects the practical application of these biosensors. In the work reported herein, we use a mimic of hemeprotein, hydroxyferriprotoporphyrin (hematin), to functionalize single-walled carbon nanotubes (SWNTs) in the presence of 1-butyl-3-methylimidazolium hexafluorophosphate ([BMIM][PF_6]) ionic liquid

[a] W. Tu, Dr. J. Lei, Prof. H. Ju
Key Laboratory of Analytical Chemistry for Life Science
(Ministry of Education of China)
Department of Chemistry, Nanjing University
Nanjing 210093 (P. R. China)
Fax: (+86) 25-8359-3593
E-mail: jpl@nju.edu.cn
hxju@nju.edu.cn

(IL), as shown in Figure 1. The resulting novel functional composite can be conveniently used for the preparation of TCA biosensors. The water-insoluble hematin leads to good stability of the biosensors.

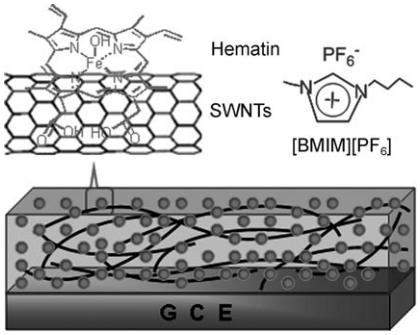

Figure 1. Schematic diagram of a porphyrin/SWNTs–[BMIM][PF_6]-modified glassy carbon electrode (GCE).

Functionalized carbon nanotubes have attracted considerable attention for various applications.[20–23] Generally, the functionalization of carbon nanotubes with porphyrin can be performed by a covalent or noncovalent route.[24–27] The latter is particularly promising because the covalent approach may cause a partial loss of the electronic properties of functionalized carbon nanotubes. The noncovalent combination of carbon nanotubes with porphyrins can undergo fast electron transfer, which leads to excellent performance of photovoltaic devices.[28,29] Some water-soluble porphyrin compounds have been assembled on carbon nanotubes for the electrochemical detection of oxygen and nitric oxide.[30,31] In this work, the water-insoluble hematin assembled on SWNTs in an IL shows direct electrochemistry corresponding to the reduction and oxidation of the Fe^{III}/Fe^{II} couple. The presence of the IL [BMIM][PF_6] enhances greatly the direct electrochemical response, which is beneficial to improving the sensitivity of the resulting biosensors.

ILs can dissolve a large number of organic electrocatalysts,[32] and have gained increasing interest in biosensing due to their wide potential window and extremely high ionic conductivity.[33–37] The water-insoluble hematin can be well dissolved in these media, which simplifies greatly the assembly of water-insoluble porphyrin on SWNTs. More significantly, the catalytic activity of porphyrin and the excellent conductivity of IL and SWNTs in the as-prepared composite film lead to a synergic effect to accelerate the reduction of TCA. Thus, besides good stability, the resulting biosensor for TCA shows much higher sensitivity than those reported previously.[9–11,17–19] The rapid response, good reproducibility, and acceptable accuracy of the proposed biosensor show its promising application in environmental monitoring and public health programs.

Results and Discussion

SEM and UV absorption characterization of porphyrin/SWNTs–[BMIM][PF_6]: The morphologies of the pristine SWNTs and porphyrin/SWNTs–[BMIM][PF_6] films were observed by scanning electron microscopy (SEM; Figure 2).

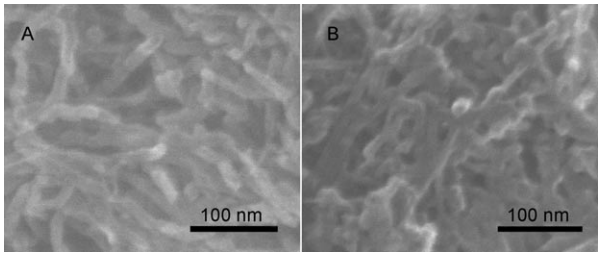

Figure 2. A) SEM images of pristine SWNTs and B) porphyrin/SWNTs–[BMIM][PF_6].

SWNTs were discernible and showed a larger diameter than the real diameter, which resulted from the aggregation of SWNTs in bundles.[38] In porphyrin/SWNTs–[BMIM][PF_6] film, the SWNTs were enwrapped by [BMIM][PF_6] due to the binding and blanketing effect of [BMIM][PF_6], which led to a slightly greater diameter than that of the pristine SWNTs and meant that the porphyrin/SWNTs were not well distinguished. Although some parts of the porphyrin/SWNTs were shown to be in close touch, they were well dispersed in the [BMIM][PF_6] to form a robust homogeneous gel for the construction of biosensors.

Figure 3 shows the UV absorption spectra of SWNTs–[BMIM][PF_6], porphyrin–[BMIM][PF_6], and porphyrin/SWNTs–[BMIM][PF_6] film formed on an indium tin oxide (ITO) surface. The SWNTs–[BMIM][PF_6] did not show obvious absorption (Figure 3, curve a). Hematin dissolved in [BMIM][PF_6] exhibited a typical Soret band absorption at 411 nm (Figure 3, curve b), characteristic of the Soret electronic absorption band of the porphyrin unit.[39] In the presence of SWNTs, the Soret band of porphyrin/SWNTs–

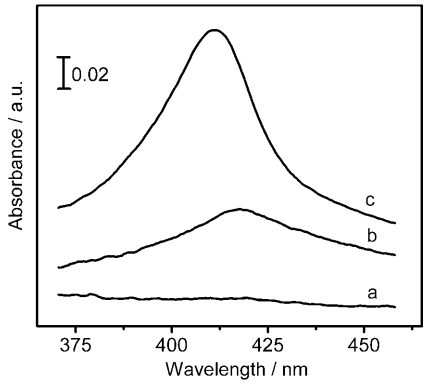

Figure 3. UV absorption spectra of a) SWNTs–[BMIM][PF_6], b) porphyrin–[BMIM][PF_6], and c) porphyrin/SWNTs–[BMIM][PF_6] confined on an ITO surface.

[BMIM][PF_6] film showed a decrease of intensity with a red shift from 411 to 418 nm (Figure 3, curve c), which indicated the formation of J-type aggregate nucleated on SWNTs.[25] This result demonstrated that hematin was successfully adsorbed on SWNTs in the presence of [BMIM][PF_6].

Electrochemical impedance spectroscopic characterization of porphyrin/SWNTs–[BMIM][PF_6]: By using the $Fe(CN)_6^{3-/4-}$ redox couple as the electrochemical probe, the Nyquist plots of different electrodes in the frequency range from 0.01 to 100000 Hz were obtained (Figure 4). At a bare

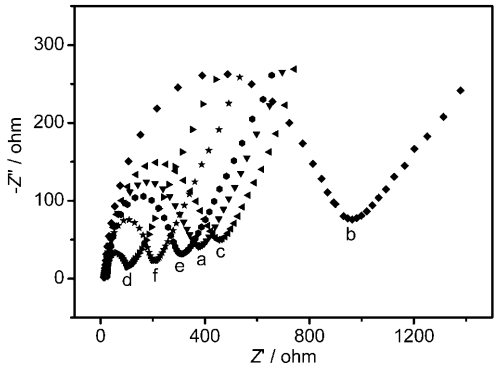

Figure 4. Electrochemical impedance spectra of a bare GCE (a) and GCEs modified with b) porphyrin, c) porphyrin–[BMIM][PF_6], d) SWNTs–[BMIM][PF_6], e) porphyrin/SWNTs, and f) porphyrin/SWNTs–[BMIM][PF_6], in 0.1 M KCl solution containing 5 mM $K_3[Fe(CN)_6]$/5 mM $K_4[Fe(CN)_6]$.

glassy carbon electrode (GCE) the redox process of the probe showed an electron-transfer resistance of about 370 Ω (Figure 4, curve a). After hematin was coated on the electrode, the resistance increased dramatically to about 960 Ω (Figure 4, curve b), which suggested that hematin film blocked the electron exchange between the redox probe and electrode surface. The presence of [BMIM][PF_6] on the hematin-coated electrode greatly improved the electron transfer. The porphyrin–[BMIM][PF_6]-modified GCE showed an electron-transfer resistance of only 450 Ω (Figure 4, curve c). On the other hand, the porphyrin/SWNTs-modified GCE showed an electron-transfer resistance of about 280 Ω (Figure 4, curve e), thus implying that the SWNTs accelerated the electron transfer due to their excellent conductivity. Compared with both porphyrin/SWNTs and porphyrin–[BMIM][PF_6]-modified GCEs, the electron-transfer resistance of 190 Ω at the porphyrin/SWNTs–[BMIM][PF_6]-modified GCE was lowest (Figure 4, curve f), and indicated a synergic effect of SWNTs and [BMIM][PF_6] in accelerating electron transfer. This effect led to very fast electron transfer of $[Fe(CN)_6]^{3-/4-}$ at the SWNTs–[BMIM]-[PF_6]-modified GCE (Figure 4, curve d). The increase of electron-transfer resistance in the presence of hematin confirmed that the porphyrin was successfully assembled on the surface of SWNTs, which resulted in the hindered pathway of electron transfer.

Electrochemical behavior of porphyrin/SWNTs–[BMIM]-[PF_6]-modified GCE: The cyclic voltammograms of bare, hematin-modified, and SWNTs–[BMIM][PF_6]-modified GCEs in phosphate-buffered saline (PBS) did not show any observable peak (Figure 5, curves a–c), whereas GCEs

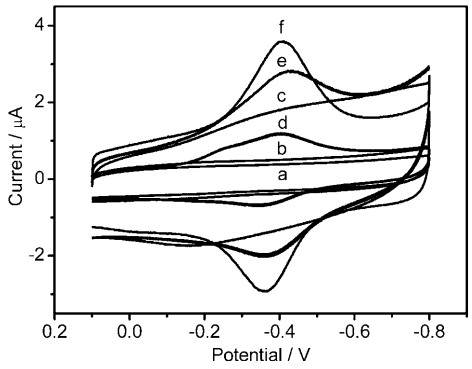

Figure 5. Cyclic voltammograms of a bare GCE (a) and GCEs modified with b) hematin, c) SWNTs–[BMIM][PF_6], d) porphyrin–[BMIM][PF_6], e) porphyrin/SWNTs, and f) porphyrin/SWNTs–[BMIM][PF_6], in PBS (0.1 M, pH 7.0) at 100 mV s^{-1}.

modified with porphyrin–[BMIM][PF_6], porphyrin/SWNTs, and porphyrin/SWNTs–[BMIM][PF_6] showed a pair of redox peaks (Figure 5, curves d–f). These peaks could be attributed to the Fe^{III}/Fe^{II} redox couple in hematin, although they could not be observed at the hematin-coated GCE due to the high electron-transfer resistance. The good solubility of hematin in [BMIM][PF_6] and the improvement of electron transfer by [BMIM][PF_6] or SWNTs led to the direct electron transfer of hematin at porphyrin–[BMIM][PF_6]- and porphyrin/SWNTs-modified GCEs. Furthermore, the porphyrin/SWNTs–[BMIM][PF_6]-modified GCE showed a couple of stable, symmetrical, and well-defined redox peaks at −0.363 and −0.404 V with a cathodic peak current of 2.07 μA, which was much larger than the 0.65 μA at porphyrin–[BMIM][PF_6]-modified GCEs and 1.28 μA at porphyrin/SWNTs-modified GCEs. The weights of coatings on the three electrodes were identical, and thus the amount of porphyrin at the porphyrin/SWNTs–[BMIM][PF_6]-modified GCE was lowest. The largest peak current, which was even greater than the sum of peak currents at the other two electrodes, further confirmed the synergic effect of SWNTs and [BMIM][PF_6] in accelerating the electron transfer between porphyrin and the GCE.

The reduction and oxidation peak currents of the porphyrin/SWNTs–[BMIM][PF_6]-modified GCE increased linearly with the scan rate in the range of 40–500 mV s^{-1}, whereas the difference of redox peak potentials showed a slight increase, which indicated a surface-controlled electrode process. With an increase of pH from 5 to 9, the redox potentials of the porphyrin/SWNTs–[BMIM][PF_6]-modified GCE shifted to more negative values and exhibited a linear relationship with slopes of −55.6 and −54.7 mV pH^{-1} for the reduction and oxidation processes, respectively. These slopes

were very close to the theoretical value of $-59.1\ mV\,pH^{-1}$ at 25 °C, thus indicating that one proton participated in the one-electron redox process.

Electrocatalytic reduction of TCA: A comparison of the electrocatalytic reduction of TCA at different electrodes in the potential range of +0.1 to −0.8 V is shown in Figure 6.

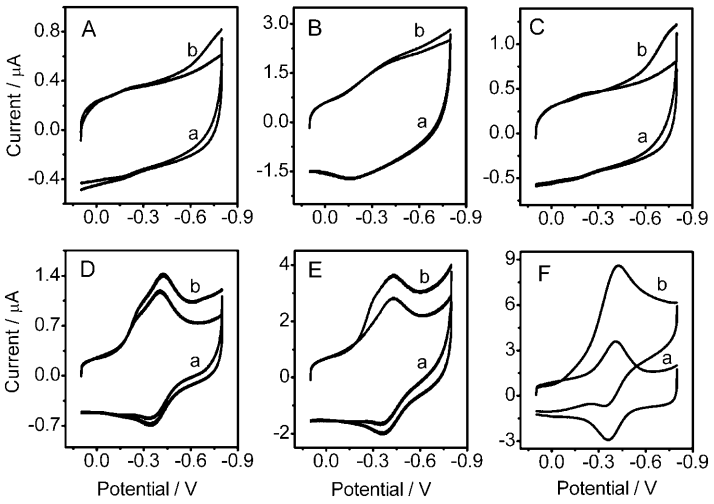

Figure 6. Cyclic voltammograms of a bare GCE (A) and GCEs modified with B) SWNTs–[BMIM][PF_6], C) porphyrin, D) porphyrin–[BMIM]-[PF_6], E) porphyrin/SWNTs, and F) porphyrin/SWNTs–[BMIM][PF_6], in a) PBS (0.1 M, pH 7.0) and b) (a) + 100 μM TCA at 100 $mV\,s^{-1}$.

When 100 μM TCA was added to PBS, no obvious reduction peak was observed at the bare and SWNTs–[BMIM][PF_6]-modified GCEs (Figure 6A and B). The cyclic voltammogram of TCA at the porphyrin-coated GCE showed a reduction process at potentials more negative than −0.45 V with a weak peak at −0.748 V (Figure 6C), which indicated a weak electrocatalysis of porphyrin toward its reduction due to the very slow electron transfer between the water-insoluble porphyrin and electrode. However, the electrocatalytic reduction peak could be observed at around −0.43 V at GCEs modified with porphyrin–[BMIM][PF_6] (Figure 6D) and porphyrin/SWNTs (Figure 6E). The electrocatalytic peak currents (the increase in the reduction peak of porphyrin) were 0.95 and 2.32 μA, which was much lower than that of 7.62 μA at the porphyrin/SWNTs–[BMIM][PF_6]-modified GCE (Figure 6F). The latter started at −0.08 V, more positive than the −0.24 and −0.20 V at porphyrin–[BMIM][PF_6]- and porphyrin/SWNTs-modified GCEs, respectively. Clearly, the electrocatalysis of porphyrin toward the reduction of TCA at the porphyrin/SWNTs–[BMIM][PF_6]-modified GCE also showed a synergic effect of porphyrin, SWNTs, and [BMIM][PF_6].

At the porphyrin/SWNTs–[BMIM][PF_6]-modified GCE the peak potential for TCA reduction was −0.40 V, which was much more positive than the −0.5 V at a water-insoluble cobalt phthalocyanine–didodecylammonium bromide–clay-modified pyrolytic graphite electrode (PGE),[40] −0.60 V at a (poly-L-lysine)–cobalt corrin vitamin B_{12} hexacarboxylic acid-modified PGE,[41] and −0.75 V at a binuclear cobalt phthalocyaninehexasulfonate sodium salt–didodecyldimethylammonium bromide-modified PGE.[42] Thus, the proposed biosensor would have a better ability to exclude the interference of other reductive species coexisting in the samples.

Condition optimization: The cyclic voltammetric performance of the porphyrin/SWNTs–[BMIM][PF_6]-modified GCE depended on the concentration of SWNTs used in the preparation of porphyrin/SWNTs–[BMIM][PF_6]. As shown in Figure 7A, with an increasing amount of SWNTs added

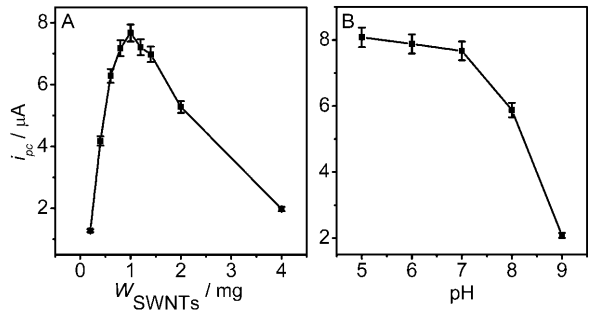

Figure 7. Effects of A) concentration of SWNTs in the preparation of the modified GCE and B) pH on the electrocatalytic peak current in 0.1 M PBS containing 100 μM TCA at 100 $mV\,s^{-1}$.

to a [BMIM][PF_6] solution (0.2 mL) of porphyrin (4 mM), the electrocatalytic current of TCA increased and reached a maximum value at 1 mg, which was attributed to the excellent electrical conductivity of SWNTs for accelerating the electron transfer between the porphyrin and GCE. However, when the amount of SWNTs was larger than 1 mg, the electrocatalytic current decreased due to the relatively decreasing amount of porphyrin assembled on SWNTs, which was a key component for the electrocatalysis. Thus, 1 mg SWNTs was added to 0.2 mL of a [BMIM][PF_6] solution of 4 mM porphyrin for the preparation of modified electrodes.

The pH value of the detection solution was also an important parameter. The electrocatalytic current of TCA decreased slowly with increasing pH value from 5 to 7, followed by a dramatic decrease on increasing the pH from 7 to 9 (Figure 7B), which indicated that a proton was necessary for the reduction of TCA.[35] The catalytic species was possibly hemin (Fe-H_2O) obtained as a result of the protonation of hematin (Fe-OH) at pH 5–7, which has a pK of ≈8. In view of the pH in biological and most environmental systems, pH 7.0 was chosen for amperometric sensing of TCA, at which the electrocatalytic peak current was 95% of that at pH 5, thus showing enough sensitivity for the amperometric detection of TCA.

Amperometric sensing of TCA: The current–time curve of the porphyrin/SWNTs–[BMIM][PF_6]-modified GCE upon successive additions of TCA at an applied potential of −0.40 V clearly illustrated that the modified GCE could re-

spond very rapidly to a change in the TCA concentration (Figure 8), producing steady signals within only 4 s. The response displayed a linear TCA concentration range from

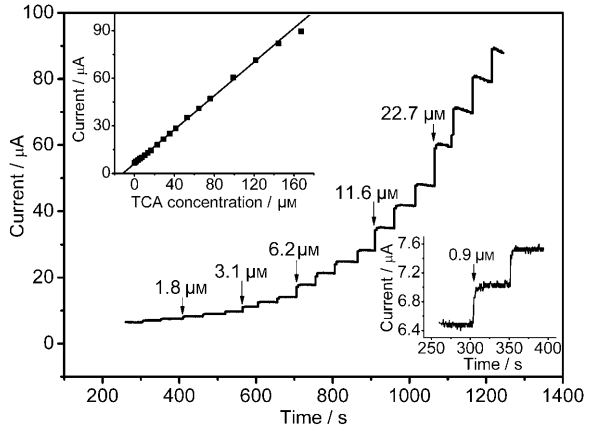

Figure 8. Successive amperometric response of a porphyrin/SWNTs–[BMIM][PF_6]-modified GCE to TCA in PBS (0.1 M, pH 7.0) at −0.40 V. Insets: linear calibration curve and amplified response.

9.0×10^{-7} to 1.4×10^{-4} M with a detection limit of 3.8×10^{-7} M at a signal-to-noise ratio of 3. The linear response range was wider than those of 3.4×10^{-3} to 7.0×10^{-2} M at a myoglobin/poly(styrenesulfonate)-modified PGE,[10] 2.0×10^{-6} to 1.2×10^{-5} M at a myoglobin/colloidal gold nanoparticles/TiO_2 sol–gel-modified GCE,[18] and 1×10^{-3} to 8×10^{-3} M at a hemin/Nafion film-modified GCE.[9] The sensitivity was $7.54\ A\,M^{-1}\,cm^{-2}$, much higher than those of $1.09\ mA\,M^{-1}\,cm^{-2}$ at a hemoglobin–chitosan–IL-modified GCE[35] and $0.35\ mA\,M^{-1}\,cm^{-2}$ at a myoglobin/poly(styrenesulfonate)-modified PGE.[10] Thus, the porphyrin/SWNTs–[BMIM][PF_6]-based biosensor for TCA had a very high sensitivity.

The TCA biosensor showed good fabrication reproducibility with a relative standard deviation of 3.56%, estimated from the slopes of the calibration plots at five freshly prepared porphyrin/SWNTs–[BMIM][PF_6]-modified GCEs. At the TCA concentrations of 5 and 100 μM, the biosensor showed good repeatability with relative standard deviations of 3.24 and 3.68% for five determinations, respectively. The batch-to-batch reproducibility showed a relative standard deviation of 4.50% for the slopes of calibration plots obtained from five independently prepared biosensors.

When the biosensor was not in use, it was stored in the shade at room temperature and tested every day. No obvious decrease in the amperometric response to TCA was observed after one week of storage. It kept 94.5% of its initial amperometric response after a month. This implied that the structure of the porphyrin/SWNTs–[BMIM][PF_6] film was very efficient for retaining the activity of porphyrin and preventing it from leaking out of the biosensor.

Interference and detection of TCA in real samples: The effects of common interfering species on the biosensor response were examined. A detection potential of −0.4 V, more positive than those applied at other amperometric TCA biosensors, avoided interference by electrochemically reducible compounds. NaCl, $MgSO_4$, KNO_3, $CuSO_4$, $AlCl_3$, NH_4Cl, Na_3PO_4, $CaCl_2$, $ZnCl_2$, ethanol, urea, methanol, sucrose, and glucose at 1000 times the concentration of TCA did not interfere with the amperometric response of TCA. Acetic acid and uric acid could be tolerated at less than 300 times the concentration of TCA. Ascorbic acid and lactic acid could be tolerated at less than 200 times the concentration of TCA. These results indicated that the amperometric biosensor had an excellent specificity for the highly sensitive detection of TCA.

The concentration of residual TCA in polluted water from the Yangzi Petrochemical Company Ltd. was detected with the proposed biosensor to be 43.1 ± 1.6 μM (five measurements) without any need of sample pretreatment except for an appropriate dilution of the sample. Due to the lack of experimental conditions available in our laboratory to perform a traditional or referee determination of TCA, recovery testing was carried out to demonstrate the validity of the proposed method. After 5.0, 30, and 100 μM of TCA were added to this sample, the obtained recoveries of TCA were 97.8 ± 3.2, 98.8 ± 3.5, and 103.6 ± 3.8%, respectively (five measurements), which indicated acceptable accuracy.

Conclusions

A novel functional composite of SWNTs with water-insoluble porphyrin has been prepared in an IL for constructing a biosensor. The porphyrin dissolved in [BMIM][PF_6] IL can be self-assembled on SWNTs by π–π noncovalent interaction, which leads to good dispersion of the SWNTs in the IL and a direct electrochemical response corresponding to the redox couple Fe^{III}/Fe^{II}. The presence of SWNTs and [BMIM][PF_6] produces a synergic effect that accelerates the electron transfer between the redox probe or water-insoluble porphyrin and the electrode. The porphyrin/SWNTs–[BMIM][PF_6]-modified GCE shows excellent electrocatalytic activity toward the reduction of TCA, producing a highly sensitive biosensor for TCA due to the synergic effect of SWNTs, [BMIM][PF_6], and porphyrin. The biosensor exhibited good analytical performance in neutral media, such as rapid electrocatalytic response, wide linear range, low detection limit, good fabrication reproducibility, detection precision and stability, excellent specificity, and acceptable accuracy. The functionalization of carbon nanotubes with water-insoluble porphyrin in an IL provides a facile way for preparing novel biofunctional materials, accelerating electron transfer, and extending the application of water-insoluble porphyrins.

Experimental Section

Materials and reagents: Hydroxyferriprotoporphyrin (hematin, 98%) was purchased from Alfa Aesar China Ltd. (China). [BMIM][PF_6] (99%) was purchased from Chemer Co. (China). SWNTs (diameter <2 nm) were

purchased from Shenzhen Nanotech Co. (China). TCA (>99%) was purchased from Shanghai Lingfeng Chemical Reagents Ltd. (China). All other chemicals were of analytical grade. Aqueous solutions were prepared with twice-distilled water. PBS solution (0.1 M) was always employed as supporting electrolyte, and was deaerated with high-purity nitrogen. The pH value of the PBS was 7.0 except where otherwise indicated.

Apparatus: SEM images were obtained by using a Hitachi S-4800 scanning electron microscope (Hitachi, Japan). UV absorption spectra were recorded with a Lambda 35 UV/Vis spectrometer (Perkin–Elmer Instruments, USA). Electrochemical impedance spectroscopic measurements were carried out on a PGSTAT30/FRA2 system (Autolab, The Netherlands) in KCl solution (0.1 M) containing $K_3[Fe(CN)_6]/K_4[Fe(CN)_6]$ (both 5 mM). The impedance spectra were recorded in the frequency range of 10^{-2}–10^5 Hz. The amplitude of the applied sine wave potential in each case was 5 mV. Cyclic voltammetric experiments were performed on a CHI 610C electrochemical workstation (CH Instruments Inc., USA), and amperometric experiments were performed on a CHI 812B electrochemical workstation (CH Instruments Inc., USA). All experiments were carried out at room temperature by using a conventional three-electrode system with a modified GCE as working electrode, a platinum wire as auxiliary electrode, and a saturated calomel electrode as reference electrode.

Preparation of modified GCEs: The GCEs (3 mm in diameter) were polished to a mirror finish with 0.1 and 0.05 μm alumina slurry on chamois leathers, and then washed ultrasonically in absolute ethanol and twice-distilled water for 2 min, respectively, and dried at room temperature. Hematin was dissolved in $[BMIM][PF_6]$ IL (5 mL) with the aid of ultrasonic agitation to give a brown solution of porphyrin (4 mM). Further, a fuscous porphyrin/SWNTs–$[BMIM][PF_6]$ gel was obtained by mixing SWNTs (1 mg) with a $[BMIM][PF_6]$ solution (0.2 mL) of porphyrin (4 mM), followed by grinding in an agate mortar for about 20 min. Then, the porphyrin/SWNTs–$[BMIM][PF_6]$ film was coated on the pretreated GCE by rubbing the electrode over the gel. To obtain a homogeneous thin gel film, the coating was further smoothed with a spatula and the modified amount was controlled to 0.5 mg by weighing. Similarly, SWNTs–$[BMIM][PF_6]$- and porphyrin–$[BMIM][PF_6]$-modified GCEs were prepared in the absence of porphyrin or SWNTs, respectively. Porphyrin- and porphyrin/SWNTs-modified GCEs were prepared by using chloroform instead of $[BMIM][PF_6]$ as solvent.

Acknowledgements

This work was supported by the Funds for Creative Research Groups (20521503), Major Research Plan (90713015), Key (20535010) and General (20745003, 20705012) Programs from the NSFC, the PhD Fund of MOE for Young Teachers (20070284052), and the Science Foundation of Jiangsu (BK2007570).

[1] J. N. Cape, S. T. Forczek, G. Gullner, G. Mena-Benitez, P. Schroder, M. Matucha, *Environ. Sci. Pollut. Res. Int.* **2006**, *13*, 276–286.
[2] C. P. Weisel, H. Kim, P. Haltmeier, J. B. Klotz, *Environ. Health Perspect.* **1999**, *107*, 103–110.
[3] H. Kim, P. Haltmeier, J. B. Klotz, C. P. Weisel, *Environ. Res.* **1999**, *80*, 187–195.
[4] *World Health Organization, Guidelines for Drinking Water Quality. Vol. 2, Health Criteria and Other Supporting Information*; 2nd ed., Geneva, **1996**, pp. 940–949.
[5] J. W. Miller, P. C. Uden, R. M. Barnes, *Anal. Chem.* **1982**, *54*, 485–488.
[6] Y. H. Wang, P. K. Wong, *Water Res.* **2005**, *39*, 1844–1848.
[7] D. O. Johns, R. L. Dills, M. S. Morgan, *J. Chromatogr. B* **2005**, *817*, 255–261.
[8] Z. Kuklenyik, D. L. Ashley, A. M. Calafat, *Anal. Chem.* **2002**, *74*, 2058–2063.
[9] A. G. de la Rosa, E. Castro-Quezada, S. Gutiérrez-Granados, F. Bedioui, A. Alatorre-Ordaz, *Electrochem. Commun.* **2005**, *7*, 853–856.
[10] H. Y. Ma, N. F. Hu, J. F. Rusling, *Langmuir* **2000**, *16*, 4969–4975.
[11] Y. L. Zhou, Z. Li, N. F. Hu, Y. H. Zeng, J. F. Rusling, *Langmuir* **2002**, *18*, 8573–8579.
[12] V. B. Kandimalla, H. X. Ju, *Chem. Eur. J.* **2006**, *12*, 1074–1080.
[13] G. Pagona, A. S. D. Sandanayaka, A. Maigné, J. Fan, G. C. Papavassiliou, I. D. Petsalakis, B. R. Steele, M. Yudasaka, S. Iijima, N. Tagmatarchis, O. Ito, *Chem. Eur. J.* **2007**, *13*, 7600–7607.
[14] Y. Xiao, V. Pavlov, B. Shlyahovsky, I. Willner, *Chem. Eur. J.* **2005**, *11*, 2698–2704.
[15] S. S. Wong, E. Joselevich, A. T. Wooley, C. L. Cheung, C. M. Leiber, *Nature* **1998**, *394*, 52–55.
[16] L. N. Wu, X. J. Zhang, H. X. Ju, *Anal. Chem.* **2007**, *79*, 453–458.
[17] W. Sun, R. F. Gao, K. Jiao, *J. Phys. Chem. B* **2007**, *111*, 4560–4567.
[18] Y. C. Li, W. W. Yang, Y. Bai, C. Q. Sun, *Electroanalysis* **2006**, *18*, 499–506.
[19] Y. H. Zhang, X. Chen, W. S. Yang, *Sens. Actuators B* **2008**, *130*, 682–688.
[20] D. Tasis, N. Tagmatarchis, A. Bianco, M. Prato, *Chem. Rev.* **2006**, *106*, 1105–1136.
[21] M. Prato, K. Kostarelos, A. Bianco, *Acc. Chem. Res.* **2008**, *41*, 60–68.
[22] Y. P. Sun, K. F. Fu, Y. Lin, W. J. Huang, *Acc. Chem. Res.* **2002**, *35*, 1096–1104.
[23] K. Balasubramanian, M. Burghard, *Small* **2005**, *1*, 180–192.
[24] D. M. Guldi, G. M. A. Rahman, F. Zerbetto, M. Prato, *Acc. Chem. Res.* **2005**, *38*, 871–878.
[25] J. Y. Chen, C. P. Collier, *J. Phys. Chem. B* **2005**, *109*, 7605–7609.
[26] D. M. Guldi, G. M. A. Rahman, M. Prato, N. Jux, S. H. Qin, W. Ford, *Angew. Chem.* **2005**, *117*, 2051–2054; *Angew. Chem. Int. Ed.* **2005**, *44*, 2015–2018.
[27] D. Baskaran, J. W. Mays, X. P. Zhang, M. S. Bratcher, *J. Am. Chem. Soc.* **2005**, *127*, 6916–6917.
[28] D. M. Guldi, G. M. A. Rahman, N. Jux, N. Tagmatarchis, M. Prato, *Angew. Chem.* **2004**, *116*, 5642–5646; *Angew. Chem. Int. Ed.* **2004**, *43*, 5526–5530.
[29] G. M. A. Rahman, D. M. Guldi, S. Campidelli, M. Prato, *J. Mater. Chem.* **2006**, *16*, 62–65.
[30] Y. Liu, Y. L. Yan, J. P. Lei, F. Wu, H. X. Ju, *Elecrochem. Commun.* **2007**, *9*, 2564–2570.
[31] W. W. Tu, J. P. Lei, H. X. Ju, *Electrochem. Commun.* **2008**, *10*, 766–769.
[32] K. E. Gutowski, G. A. Broker, H. D. Willauer, J. G. Huddleston, R. P. Swatloski, J. D. Holbrey, R. D. Rogers, *J. Am. Chem. Soc.* **2003**, *125*, 6632–6633.
[33] F. Zhao, X. E. Wu, M. K. Wang, Y. Liu, L. X. Gao, S. J. Dong, *Anal. Chem.* **2004**, *76*, 4960–4967.
[34] N. Maleki, A. Safavi, F. Tajabadi, *Anal. Chem.* **2006**, *78*, 3820–3826.
[35] X. B. Lu, J. Q. Hu, X. Yao, Z. P. Wang, J. H. Li, *Biomacromolecules* **2006**, *7*, 975–980.
[36] B. K. Price, J. L. Hudson, J. M. Tour, *J. Am. Chem. Soc.* **2005**, *127*, 14867–14870.
[37] T. Li, B. L. Li, S. J. Dong, E. Wang, *Chem. Eur. J.* **2007**, *13*, 8516–8521.
[38] V. Georgakilas, K. Kordatos, M. Prato, D. M. Guldi, M. Holzinger, A. Hirsch, *J. Am. Chem. Soc.* **2002**, *124*, 760–761.
[39] R. Chitta, A. S. D. Sandanayaka, A. L. Schumacher, L. D. Souza, Y. Araki, O. Ito, F. D. Souza, *J. Phys. Chem. C* **2007**, *111*, 6947–6955.
[40] N. F. Hu, J. F. Rusling, *Anal. Chem.* **1991**, *63*, 2163–2168.
[41] D. L. Zhou, C. K. Njue, J. F. Rusling, *J. Am. Chem. Soc.* **1999**, *121*, 2909–2914.
[42] X. E. Jiang, L. P. Guo, X. G. Du, *Talanta* **2003**, *61*, 247–256.

Received: August 26, 2008
Published online: December 4, 2008

